Available online at www.sciencedirect.com
SCIENCE DIRECT
International Journal of Heat and Fluid Flow 27 (2006) 259–266
International Journal of HEAT AND FLUID FLOW
www.elsevier.com/locate/ijhff

Sintered porous medium heat sink for cooling of high-power mini-devices

G. Hetsroni *, M. Gurevich, R. Rozenblit

Department of Mechanical Engineering, Technion—Israel Institute of Technology, 32000 Haifa, Israel

Received 4 September 2004; received in revised form 7 August 2005; accepted 18 August 2005
Available online 13 October 2005

Abstract

Heat transfer and pressure drop in a rectangular channel with sintered porous inserts, made of stainless steel of different porosity, were investigated experimentally. Heat flux up to 6 MW/m^2 was removed experimentally by using porous samples with porosity 32% and average pore diameter 20 μm. Under this experimental condition, the difference between the temperatures of the wall and the bulk water did not exceed of 55 K with a pressure drop of 4.5 bars. The generalization of data on heat transfer in a low porosity sintered stainless steel media, based on the permeability as scale of length and the effective thermal conductivity, was considered. An estimate of a heat sink efficiency using sintered porous material for cooling high-power mini-devices and comparing it with one for such modern porous media as compressed aluminum foams was done.

Keywords: Sintered medium; Porous; Heat transfer; Enhancement; Drag reduction

1. Introduction

The problem of dissipating high heat fluxes has received much attention due to its importance in applications such as micro-porous heat exchanger, cooling of electronic equipment (mirrors in powerful lasers, phased-array radar systems), industrial furnaces, fixed-bed nuclear propulsion systems and many others. The most effective way of cooling is pumping liquid inside these devices through microchannels or porous medium. (Hwang and Chao, 1994) analyzed the enhancement of heat transfer in sintered porous channels for both thermal entrance and thermally fully developed regions. The two channels of $5 \times 5 \times 1$ cm were made of sintered bronze beads with two different mean diameters, $d = 0.72$ and 1.59 mm. The local wall temperature distribution, inlet and outlet pressures and temperatures, and heat transfer coefficients were measured for heat fluxes from 0.8 to 3.2 W/cm^2 with air velocity ranging from 0.16 to 5 m/s and the air pressure from 1 to 3 bar. The fully developed Nusselt numbers were analyzed theoretically by using a non-Darcy, two-equation flow model. Heat transfer between the solid and fluid phases was modeled as a function of Reynolds number. A wall function was introduced to model the transverse thermal dispersion process for the wall effect on the lateral mixing of the fluid. (Jiang et al., 2004a) investigated experimentally heat transfer in sintered porous plate with water and air forced convection. The effects of fluid velocity, particle diameter, type of porous medium (sintered or non-sintered), and fluid properties, on the heat transfer enhancement were investigated. The results showed that the convection heat transfer in the sintered porous plate channel was more intense than in the non-sintered porous plate channel, due to the reduced thermal contact resistance and the reduced porosity near the wall in the sintered material, especially for convection heat transfer of air. For the tested conditions, the local heat transfer coefficients in the sintered porous plate channels were increased up to 15 times for water and 30 times for air. However, the estimated maximal value of the heat flux dissipated in this setup does not exceed 0.9 MW/m^2 at pressure drop per unit length of 1.29 MPa/m at a Reynolds

* Corresponding author. Tel.: +972 48 292058; fax: +972 48 238101.
E-mail address: hetsroni@tx.technion.ac.il (G. Hetsroni).

0142-727X/$ - see front matter © 2005 Elsevier Inc. All rights reserved.
doi:10.1016/j.ijheatfluidflow.2005.08.005

Nomenclature

C_p	specific heat
D	hydraulic diameter
h	average heat transfer coefficient
I_C	inertial coefficient
K	permeability
$\dot{m}$	flow rate
q	heat flux
R_{th}	thermal resistance
T	temperature
S	area
U	average liquid velocity
W	power

Greeks

ε	volume fraction
κ	thermal conductivity
ν	kinematic viscosity
ρ	density

Subscripts

f	fluid
fill	filled
in	inlet
out	outlet
s	solid
w	wall

number $Re = 2500$ in single phase water flow. Experimental studies on the effect of compression and pore size variations on the liquid flow characteristics and heat transfer have been performed by Boomsma and Poulikakos (2002) and Boomsma et al. (2003a) regarding the initially open-cell metal foam with an average cell diameter of 2.3 mm. They showed the compressed open-cell aluminum foam heat exchangers had thermal resistances that were two or three times lower than the best commercially available heat exchanger with the same pumping power.

Most of theoretical models and numerical simulations (Hwang and Chao, 1994; Rosenfeld and North, 1995; Raffray and Pulsifer, 2003; Jiang et al., 2004b) used a particle diameter as one of the basic parameters for calculating both heat transfer and friction in the porous medium of cooling systems. Frequently, advanced electronics, optics, nuclear equipment and high frequency microwaves systems require cooling of some devices at a heat flux of about 5–30 MW/m^2. To meet this demand the porous medium of the heat exchangers has to be compressed, thus the spherical particles are distorted and agglomerated. In this case a model for numerical simulations and practical calculations needs somewhat other approaches and require an extension of experimental base to provide the necessary background.

The aim of this research is to study experimentally the effect of sintered medium porosity on the heat transfer and pressure drop in cooling devices at high heat fluxes, and to compare the performance of such heat sink with other high effective heat exchangers based on the porous material.

2. Experimental apparatus and procedure

2.1. Experimental apparatus

The test loop is depicted schematically in Fig. 1. Thoroughly filtered water was used in it as the coolant. The water was supplied to the test section from the entrance tank, 1, by a gear pump, 2. The flow rate was regulated by the valve, 3. Two pressure and temperature measure-

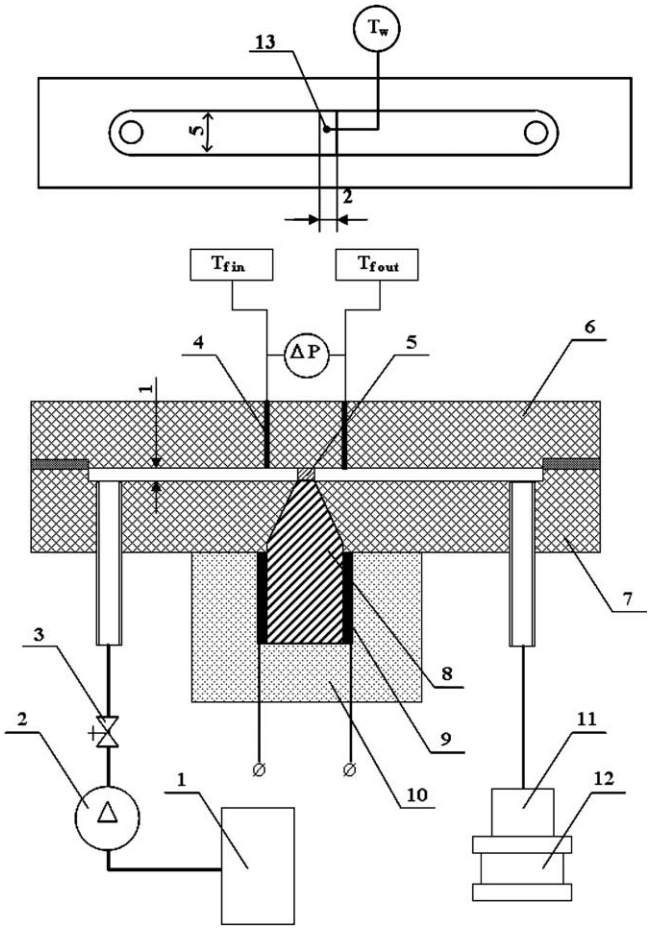

Fig. 1. Schematic diagram of the experimental facility. 1. Entrance tank, 2. Pump, 3. Control valve, 4. Temperature and pressure measurements ports, 5. Sample of porous medium, 6. Top of test section, 7. Housing. 8. Copper rod, 9. Two heaters, 10. Insulation, 11. Exit tank, 12. Electronic scales, 13. Thermocouple for measurement of the cooper rod surface temperature.

ments ports, 4, on both sides of the porous insert, 5, were bored in the top, 6, of the test section. The inlet and outlet temperatures of the working fluid were measured with 0.3 mm type T thermocouples. The pressure drop between the inlet and the outlet ports was measured by a pressure transducer. The rectangular channel of cross section 5×1 mm and the length of 70 mm was milled in the top of the lower housing block, 7. The porous insert of width 5 mm, length 2 mm and of 1 mm thickness was placed in the channel, occupying the entire cross-section. The heat was supplied to the porous sample through a copper rod, 8, with heated surface at its upper end of 5×2 mm. The rectangular basis of the rod was heated by controlled heater block, 9, attached to both sides of the rod basis and enclosed by insulation, 10. The heater could supply power up to 1.0 kW. The water flow rate was measured by weighing method using the exit tank, 11, standing on an electronic scale, 12. The temperature of the top of the rod was measured by 0.3 mm type T thermocouple, 13, inserted into the cooper, 0.5 mm beneath the porous layer.

2.2. Test samples

Stainless steel sintered material was used as a porous medium in the model of the heat sink. Applied porous media is manufactured from special grades of atomized metal powders. The 316LSS powders have rounded irregular shaped particles that are compacted prior to sintering in order to interlock the particles. The initial powder particle size controls the pore size and distribution when sintered to a specified density. The permeability is related to the pore size and pore distribution. Material properties such as thermal conductivity, thermal expansion and density are highly dependent on the porosity and generally decrease as porosity increases.

Two kinds of samples with different average pore diameter of 20 μm and 60 μm were studied. The porosities of the porous material were calculated by weighing them and comparing the density to that of solid 316 stainless steel. The structure of sintered material with average pore diameter of 20 μm is presented in Fig. 2. The samples were cut by the EDM (Electric Discharge Machining) method aiming at having open pores at the interface of porous layer. Table 1 lists the corresponding flow properties of the two porous media made of sintered stainless steel.

2.3. Procedure

All measurements were performed under steady state conditions. Each experiment was run for several minutes until the fluid and thermal regimes inside of porous layer became stabilized. The experiments were carried out in the range of average liquid velocity $0.2 \leqslant U \leqslant 1.5$ m/s in the channel with the porous insert. The range of heat flux was $0.1 \leqslant q \leqslant 0.6$ kW/cm^2. Under these experimental conditions the Reynolds number $Re = \frac{UD}{\nu}$ (D is the hydraulic diameter of the channel; ν is the kinematic viscosity) varied

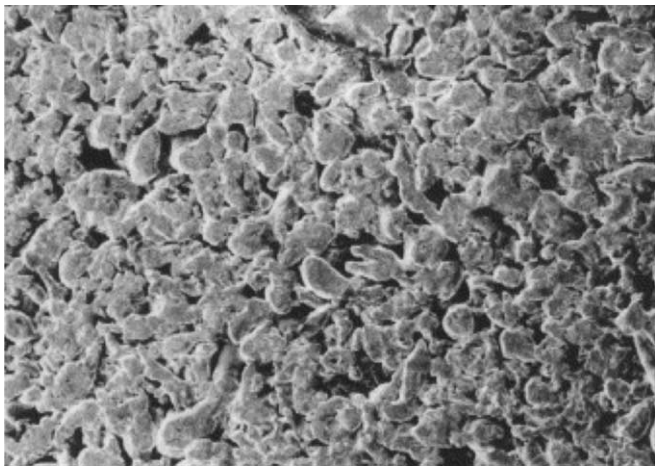

Fig. 2. Sample of sintered porous material. Real size is 3.0×2.2 mm.

Table 1
Physical parameters for sintered stainless steel media

Parameter	Sample	
Average pore diameter, μm	20	60
Porosity, ε, %	32	44
Permeability, $K \times 10^{10}$, m^2	0.215	9.6
Uncertainty of K value, %	6.45	4.11
Form coefficient, $C \times 10^{-5}$, m^{-1}	2.67	0.99
Uncertainty of C value, %	3.54	2.83

in the range $200 \leqslant Re \leqslant 2800$. The combination of values of the heat flux and velocity was varied in such a way that in the test section the flow was always single phase.

Heat flux q on the surface of the heater adjacent to the porous sample may be calculated by dividing the experimental value of the power $N = \dot{m}C_p(T_{f,out} - T_{f,in})$ convected by the fluid in the mini-channel, on the area S of the heater top (it is valid if longitudinal diffusion in the fluid is negligible). Under these measurements thermocouples have to be next to the porous sample aiming reduce the effect of heat, emanating from the housing wall, to a negligible level (less than 1%). Hence

$$q = \frac{\dot{m}C_p(T_{f,out} - T_{f,in})}{S} \tag{1}$$

where $\dot{m}$ is the flow rate, C_p is the specific heat, $T_{f,out}$ and $T_{f,in}$ are the inlet the outlet temperatures of the liquid measured by thermocouples, S is the area of the heater top.

The average heat transfer coefficient is defined as

$$h = \frac{q}{(\bar{T}_W - \bar{T}_f)} \tag{2}$$

where $\bar{T}_W$ is the average wall temperature measured by the thermocouple, $\bar{T}_f$ is the average value of the fluid temperature, calculated as the mean of the inlet $T_{f,in}$ and the outlet, $T_{f,out}$, temperatures of the liquid in the test section. All thermophysical parameters of the water, needed for evaluation of the heat transfer coefficient and Reynolds numbers, were determined at the same temperature $\bar{T}_f$.

2.4. Experimental uncertainty

The flow rate of the water $\dot{m}$ was controlled by adjusting the voltage of a gear pump and was measured by the weighing method with an uncertainty of ±0.2%. The inlet and outlet temperatures of the working fluid were measured by 0.3 mm type T thermocouples. These thermocouples were specially calibrated in a narrow temperature range of 25–40 °C with an uncertainty of 0.1 K. The temperature of the heated surface was measured by the same type of thermocouple. This thermocouple and the data acquisition system were calibrated at the steam point and ambient water temperature, and yield uncertainty values within 0.3 K at these two conditions. In order to calculate the deviations associated with the measurement of various quantities, readings were taken for a few runs every 2 min over a period of 20 min. The error in determining the average heat transfer coefficient h, according to Eqs. (1) and (2), is formed from an estimation of the measurements errors of the following values: $\dot{m}$—mass flow rate; $T_{f,out} - T_{f,in}$—difference between outlet and inlet temperatures of the liquid; $\bar{T}_W - \bar{T}_f$—difference between the averaged value of the wall and the liquid temperatures. For each kind of porous samples at a given heat flux the uncertainty is higher at the higher values of flow rate due to the small temperature difference between the outlet and inlet water temperatures. Therefore, an uncertainty estimate of heat transfer coefficient is done at the highest value of flow rate for the sample of 20 μm average pore diameter. The uncertainty of these components (Table 2) for an estimation of an error measurement of heat transfer coefficient was obtained according to the standard Guide to the Expression of Uncertainty of Measurement, 1995.

The uncertainties in determining the thermal conductivity of the cooling water and hydraulic diameter are estimated as 0.4% and 2.0%, respectively. Therefore, the uncertainties of the values of heat transfer coefficient h (Table 2) and the Nusselt number $Nu = hD/k_f$ are within 13.1% and 13.3%, respectively.

The pressure drop between the inlet and the outlet of the test section was measured by means of a pressure transducer with an uncertainty of 1.5%. The data were collected by a 12-bit 1 MHz acquisition system with an uncertainty of ±0.025% FS. The pressure drop measurements were performed both with and without the thermocouples inserted through the ports in the channel, in order to determine their effect on the measurements. The analysis showed that the pressure readings in both cases were within the uncertainty. The data on the uncertainty is generalized in Table 3.

3. Results and discussion

3.1. Pressure drop

A series of experiments were performed on this test section with a porous material made of stainless steel. The pressure difference produced by the porous insert ΔP was computed by subtracting the pressure drop ΔP_{clear} of the channel without the insert from the pressure drop ΔP_{fill} of the channel with porous insert

$$\Delta P = \Delta P_{fill} - \Delta P_{clear} \tag{3}$$

Experimental value of the Darcy velocity was computed for each pressure drop by dividing the flow rate $\dot{m}$ by the cross section area of the channel S_c (1 × 5 mm) and liquid density ρ

$$U = \dot{m}/\rho S_c \tag{4}$$

The pressure drops for the channels with two kinds of porous inserts and clear channel are shown in Fig. 3. It can be seen that the pressure drop for the clear channel is not more than a few percent of the pressure drop in the channels with insert.

The modified Darcy equation (5) was used to determine the permeability, K, and form coefficient, C, for each sample

$$\frac{\Delta P}{L} = \frac{\mu}{K} U + \rho C U^2 \tag{5}$$

where μ and ρ are dynamic viscosity and density of fluid respectively.

Fig. 4 shows the pressure drop per the unit length for the two porous inserts. It can be seen that the pressure drop in the porous material with 20 μm pore diameter is more than twice as large as that for the porous material of 60 μm.

The permeability and form coefficient for each porous layer were obtained directly from fitting (Antohe et al., 1996) by quadratic polynomial. The uncertainty determination of permeability and form coefficient was performed according to algorithm given in Antohe et al. (1997). This method was successfully employed (Boomsma and Pouli-

Table 2
Summary of standard uncertainty components of heat transfer coefficient ($\dot{m} = 4.06 \times 10^{-3}$ kg s^{-1}, $d_p = 20$ μm)

Standard uncertainty component $u(x_i)$	Source of uncertainty	Value of standard uncertainty $u(x_i)$	$c_i \equiv \partial h/\partial x_i$	$\frac{u(x_i)\lvert c_i\rvert}{h}$
$u(\dot{m})$	Flow rate	2.8×10^{-6} kg/s	$4.2 \times 10^8 \frac{T_{f,out} - T_{f,in}}{\bar{T}_{W,IR} - \bar{T}_f}$	6.91×10^{-4}
$u(T_{f,out} - T_{f,in})$	Measured difference between inlet and outlet liquid temperatures	0.2 K	$4.2 \times 10^8 \frac{\dot{m}}{\bar{T}_{W,IR} - \bar{T}_f}$	6.08×10^{-2}
$u(T_{W,IR} - T_f)$	Measured difference between the wall and the liquid temperatures	0.4 K	$4.2 \times 10^8 \frac{\dot{m}(T_{f,out} - T_{f,in})}{(\bar{T}_{W,IR} - \bar{T}_f)^2}$	8.28×10^{-3}

$u_c(h)/h = 6.13 \times 10^{-2}$; $h = 1.16 \times 10^5$ W/m^{2}K; degrees of freedom −8; $v_{eff}(h) = 15$; $k = 2.13$; $U_{95} = ku_c(h)$; $U_{95}(h)/h = 0.131$.

Table 3
Experimental uncertainties (95% confidence level)

NN	Parameter	Symbol	Uncertainty, %
1	Heat transfer coefficient	h	13.1
2	Nusselt number	Nu	13.3
3	Nusselt number	Nu_K	14.1
4	Mass flow rate	$\dot{m}$	0.2
5	Cross-section area	S_c	2.0
6	Fluid velocity	U	2.0
7	Reynolds number	Re	3.1
8	Reynolds number	Re_K	5.7

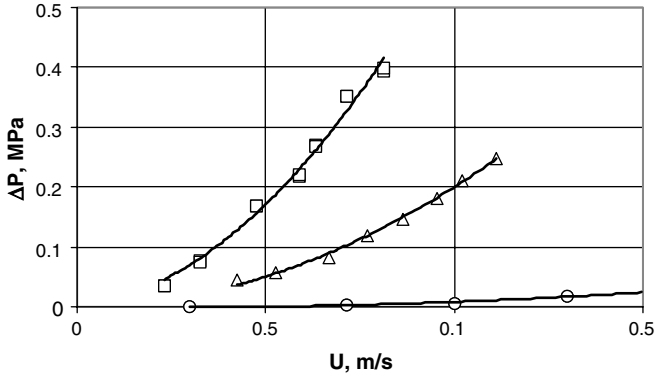

Fig. 3. Pressure drops for the channels with two kinds of porous inserts and clear channel. Hereafter symbols are according to the average pore diameter: □, 20 μm; △, 60 μm; ○, clear channel.

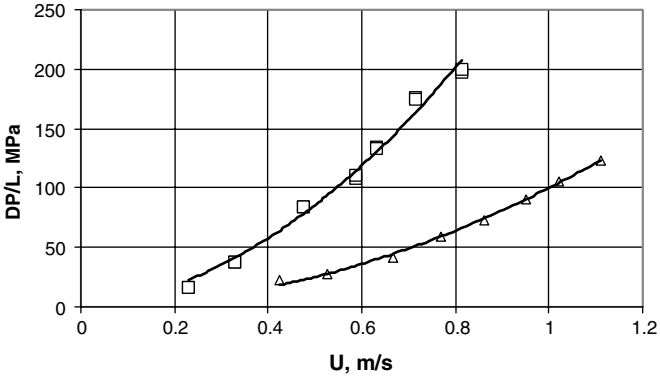

Fig. 4. Pressure drops on the length unity for the two porous inserts.

kakos, 2002) to the determination of an uncertainty of flow parameters in compressed samples of open porous foams. The magnitudes of these parameters for sintered porous material have been listed in Table 1.

3.2. Heat transfer

Fig. 5 shows the value of the heat flux, removed by a porous insert of 1 mm thickness, depending on the Reynolds number of the coolant $Re = \frac{UD}{\nu}$ (where U is liquid velocity in the channel with insert; D is hydraulic diameter of the channel; ν is kinematic viscosity). The value of the heat flux was determined according to Eqs. (1) and (2).

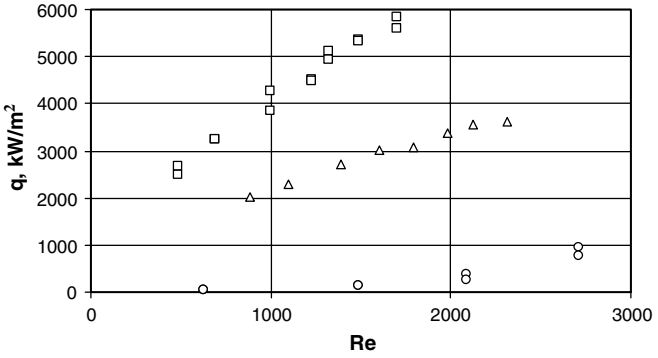

Fig. 5. Heat flux as a function of the Reynolds number.

We can see that dissipation of heat flux up to 6000 kW/m^2 was obtained, experimentally, in the range of Reynolds numbers in laminar flow regime. Under these conditions the difference between the temperatures of the wall and the water does not exceed 55 K.

The relation between the Nusselt number $Nu = \frac{hD}{k_f}$ (where h is the heat transfer coefficient; D is hydraulic diameter of the channel; k_f is the thermal conductivity of the liquid) and the Reynolds number in Fig. 6 is similar to the previous graph, because we used the same hydraulic diameter for the two kinds of porous layer with different parameters. It means that the hydraulic diameter is not a proper parameter to generalize the data for heat transfer in a porous medium.

To generalize the heat transfer data, we have to apply dimensionless numbers developed on the basis of the properties of the porous material, such as the effective characteristic size $\sqrt{K}$ and effective thermal conductivity κ_{eff} of the porous layer.

A simple estimation (Kaviany, 1995) of the effective thermal conductivity of a fluid filled porous media can be made by accounting for the volume fraction of each component:

$$k_{\text{eff}} = \varepsilon k_f + (1-\varepsilon)k_s \tag{6}$$

where ε is the porosity of porous material, k_f and k_s are thermal conductivities of the fluid and the solid phases, respectively. Thermo-physical properties of of stainless

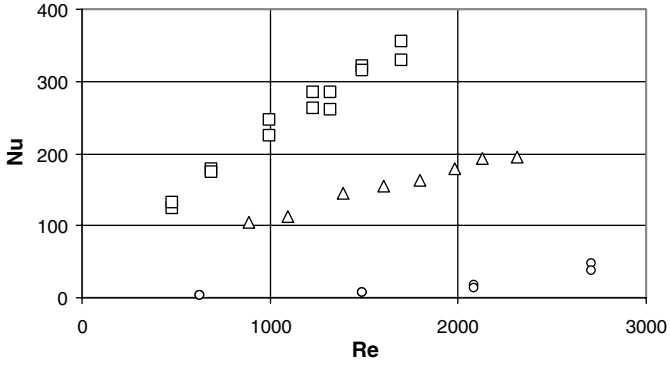

Fig. 6. Nusselt number as a function of the Reynolds number based on hydraulic diameter.

steel used in the calculation are: density 7960 kg/m^2, thermal conductivity 16.3 W/mK.

This equation is exact only if stagnant fluid and solid constitutions are placed parallel to each other. It does not account for natural convection between the solid to the fluid phases, contact resistance between packed particles or cells, radiation, or distinct structural features. Definition of effective thermal conductivity according to the Eq. (6) has some assumptions that can be formulated (Boomsma and Poulikakos, 2001) as follows:

1. The porous medium is uniform, or the porosity variation can be accurately calculated.
2. Natural convection and radiation heat transfer effects inside the porous medium can be neglected.
3. The physical properties of the solid and fluid phases remain constant throughout the temperature range.
4. The solid and fluid phases are in local thermal equilibrium.

The first two assumptions are good enough for the liquid flowing slowly through the porous medium with relatively low permeability. Amiri and Vafai (1994) extensively studied the validity of the assumption of the local thermal equilibrium. They found that the local thermal equilibrium assumption worked best, as perhaps expected, with slow moving or stagnant flows, which are commonly found in porous media with relatively low permeability.

Hence, these assumptions are well suited for heat sinks of high power devices, where porous media (sintered material or metal foam) should be compressed for an extension of heat transfer area, whereas the liquid velocity should be low because of very high pressure drops.

Closer examination of the determination of thermal and hydraulic parameters was done by Boomsma et al. (2003b) and Boomsma and Poulikakos (2001) by modeling the flow through a porous medium with a well defined structure. This approach entailed modeling idealized open cell metal foam based on a fundamental periodic unit of eight cells and solving the flow through the three-dimensional cellular unit. The foam structure was represented with cylindrical ligaments, which attach to cubic nodes at their centers. The authors showed that despite the high porosity of the foam, the heat conductivity of the solid phase controls the overall effective thermal conductivity to a large extent.

Under conditions of sintered porous material, data on heat transfer based on the permeability as length scale and effective heat conductivity, defined on the basis of simple estimation (6) of the thermal conductivity, should be considered.

The experimental data on the heat transfer in porous medium is presented as a relation between the Reynolds number $Re_K = \frac{U\sqrt{K}}{\nu}$ and Nusselt number $Nu_K = \frac{h\sqrt{K}}{k_{\text{eff}}}$ in Fig. 7. It can be seen that graph in these coordinates represents a single common curve. Such presentation makes it possible to generalize the data and estimate the heat transfer characteristics for porous cooling in the channel of different hydraulic diameter filled with porous material.

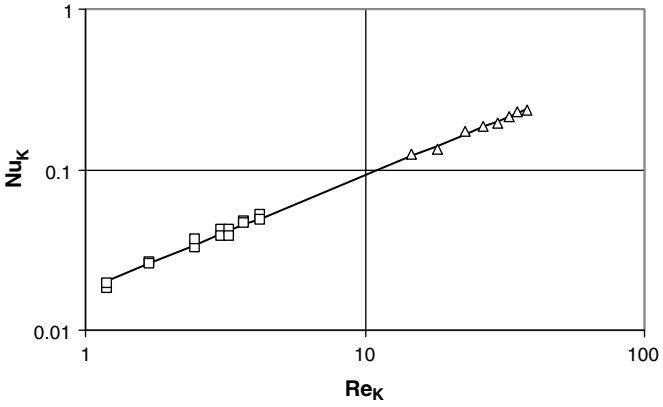

Fig. 7. Generalization of data on heat transfer in a low porosity sintered stainless steel media.

3.3. Heat sink performance

Tzeng and Ma (2004) showed that thermal characteristics of sintered porous heat sinks are better than those for traditional copper and aluminum heat sinks by experimental investigation. Now we can compare an efficiency of using sintered porous material for cooling high power mini-devices with an efficiency (Boomsma et al., 2003a) of such modern porous media as aluminum compressed foams.

A heat sink performance is characterized by the j-Colburn factor:

$$j = StPr^{2/3} \tag{7}$$

where $St = \frac{Nu}{RePr}$ is the Stanton number and Pr is the Prandtl number based on the liquid properties. This factor gives the ratio of the convection heat transfer to the required flow rate in the heat sink for different coolants. Fig. 8 shows the value of the Colburn factor depending on the Reynolds number $Re_K = \frac{U\sqrt{K}}{\nu}$ for the channel with two kinds of sintered porous material. The values of j-Colburn factor

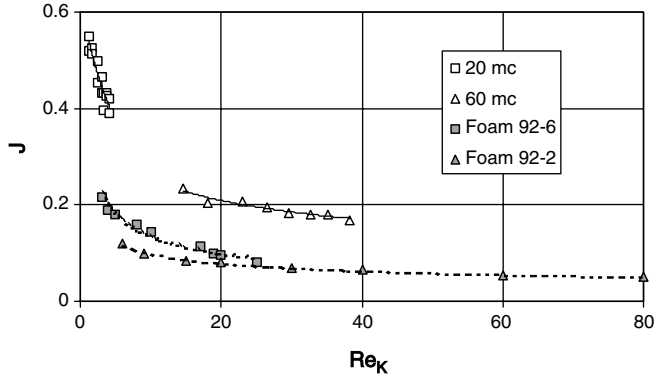

Fig. 8. Colburn factor depending on the Reynolds number based on permeability.

(Fig. 8) are highest for the porous material with average pore diameter of 20 μm at very low values of Reynolds number Re_K. Further rise in Re_K for such a sample was limited by a sharp increase in the pressure drop. The heat sink based on the porous sintered material with average pore diameter of 60 μm shows lower magnitude of j-Colburn factor, but it is observed in the extended range of Re_K. Clearly that the metal foam with very high initial porosity, even compressed, yields low j-Colburn values. It is of interest to compare the performance of this heat sink with one of the modern high-efficiency heat exchangers (Boomsma et al., 2003a) made from aluminum foam. The original open-cell foam has porosity of about 92% with an average cell diameter of 2.3 mm. The surface area of the porous insert was increased by compressing the original foam. We used for comparison their experimental data for two kinds of aluminum foam with compression ratio of 2 and 6 and the measured porosity of about 87% and 67%, respectively. The magnitudes of Colburn factor j for aluminum foam are presented also in the Fig. 8. It can be seen that the magnitude of the Colburn factor j for sintered porous stainless steel material with average pore diameter of 20 and 60 μm is at least twice that for the aluminum foam with compression ratio of 2 and 6. However this advantage of the sintered stainless steel heat sink over the aluminum foam is accomplished by a drastic increase in the pumping power W_P, or conversely there is a considerable increase in the value of the thermal resistance R_{th} with the same pumping power W_P. Hence, the effectiveness of using porous materials for cooling high-power micro-devices should be also examined in terms of a relation between the pumping power $W_P = \Delta PQ$ (here ΔP is the pressure drop across the porous insert, and Q is the volumetric flow rate of the coolant passing through the heat sink) and any thermal characteristics of the heat sink. Frequently, the value of a thermal resistance $R_{th} = \Delta T/W$ (here $\Delta T = \bar{T}_W - \bar{T}_f$ is the difference between temperatures of the and mean liquid temperature and $W = \dot{m}C_p(T_{f,out} - T_{f,in})$ is the dissipated heat) is used as such parameter. Fig. 9 demonstrates the relation between the power W_P of the cooling system and thermal resistance R_{th} for both the sintered porous heat sinks and the samples of compressed aluminum foam. It can be seen that thermal resistance R_{th} of compact heat exchangers with porous foam are well below those with sintered inserts at the same value of the power W_P of the cooling system. The decrease in the magnitude of the thermal resistance for the heat exchangers on porous sintered materials requires using high-pressure pumps, resulting in an increase in power supply on the pumping and complication of the heat exchanger design. That is why sintered porous heat sinks are effective for cooling mini-devices with very high heat release without strong limitation on pumping power and the overall dimensions of cooling system.

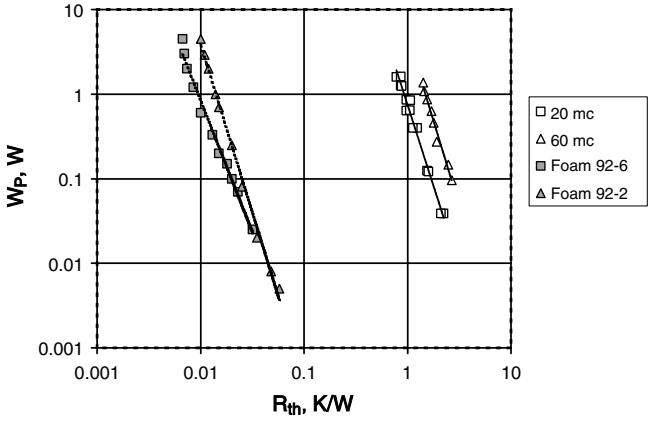

Fig. 9. Pumping power W_P vs. thermal resistance R_{th}.

4. Conclusion

A heat sink, based on porous stainless steel, for cooling mini-devices was investigated experimentally.

The heat flux up to 6000 kW/m^2 was removed by using porous samples with porosity 32% and average pore diameter 20 μm. Under the experimental conditions, the difference between the temperatures of the wall and the inlet water did not exceed of 55 K and the pressure drop was 4.5 bar.

Data on heat transfer in a low porosity sintered stainless steel media was analyzed based on the permeability as the length scale and the effective thermal conductivity.

An estimate of an efficiency of sintered porous heat sink and the comparison with an aluminum compressed foams one clearly show that such heat sink gives very high value of the heat transfer performance, whereas it is accomplished by a drastic increase in the pumping power. It means that the principal use of the sintered porous stainless steel heat sink is in mini-devices of high-power with no limitation on pumping power.

Acknowledgements

This research was supported by the Council for Higher Education, by the IAEA Soreq. R. Rozenblit was supported by a joint grant from the Center for Absorption in Science of the Ministry of Immigrant Absorption and the Committee for Planning and Budgeting of the Council for Higher Education under the framework of the KAMEA PROGRAM.

References

Amiri, A., Vafai, K., 1994. Analysis of dispersion effects and non-thermal equilibrium, non-Darcian, variable porosity incompressible flow through porous media. International Journal of Heat and Mass Transfer 37, 939–954.

Antohe, B.V., Lage, J.L., Price, D.C., Weber, R.M., 1996. Numerical characterization of micro heat exchangers using experimentally tested porous aluminum layers. International Journal of Heat and Fluid Flow 17, 594–603.

Antohe, B.V., Lage, J.L., Price, D.C., Weber, R.M., 1997. Experimental determination of permeability and inertia coefficients of mechanically

compressed aluminum porous matrices. Journal of Fluid Engineering 119, 404–412.

Boomsma, K., Poulikakos, D., 2001. On the effective thermal conductivity of a three-dimensionally structured fluid-saturated metal foam. International Journal of Heat and Mass Transfer 44, 827–836.

Boomsma, K., Poulikakos, D., 2002. The effects of compression and pore size variations on the liquid flow characteristics in metal foams. Journal of Fluids Engineering—Transactions of the ASME 124, 263–272.

Boomsma, K., Poulikakos, D., Zwick, F., 2003a. Metal foams as compact high performance heat exchangers. Mechanics of Materials 35, 1161–1176.

Boomsma, K., Poulikakos, D., Ventikos, Y., 2003b. Simulations of flow through open cell metal foams using an idealized periodic cell structure. International Journal of Heat and Fluid Flow 24, 825–834.

Guide to the Expression of Uncertainty of Measurement, 1995. International Organization for Standardization, Geneva, Switzerland. ISBN 92-67-10188-9.

Hwang, G.J., Chao, C.H., 1994. Heat transfer measurement and analysis for sintered porous channels. Journal of Heat Transfer 116, 456–464.

Jiang, P.X., Li, M., Lu, T.J., Yu, L., Ren, Z.P., 2004a. Experimental research on convection heat transfer in sintered porous plate channels. International Journal of Heat and Mass Transfer 47, 2085–2096.

Jiang, P.X., Li, M., Ma, Y.C., Ren, Z.P., 2004b. Boundary conditions and wall effect for forced convection heat transfer in sintered porous plate channels. International Journal of Heat and Mass Transfer 47, 2073–2083.

Kaviany, M., 1995. Principles of heat transfer in porous media, Second ed. Springer-Verlag, New York.

Raffray, A.R., Pulsifer, J.E., 2003. MERLOT: a model for flow and heat transfer through porous media for high heat flux applications. Fusion Engineering and Design 65, 57–76.

Rosenfeld, J.H., North, M.T., 1995. Porous media heat exchangers for cooling of high-power optical components. Optical Engineering 34, 335–341.

Tzeng, S.C., Ma, W.P., 2004. Experimental investigation of heat transfer in sintered porous heat sink. International Communications in Heat and Mass Transfer 31, 827–836.